Laser induced graphene-based glucose biofuel cell

Md Faruk Hossain (IEEE member), Gymama Slaughter (Senior IEEE member)
Center for Bioelectronics, Department of Electrical and Computer Engineering, Old Dominion University, Norfolk, VA-23528, USA.

***Abstract*— A glucose biofuel cell is presented using laser induced 3D graphene (LIG) substrate integrated with catalytic active nanomaterials for harnessing the biochemical energy of glucose. The LIG anode comprised glucose dehydrogenase immobilized on reduced graphene oxide and multiwalled carbon nanotubes (RGO/MWCNTs) nanocomposite for glucose oxidation. The LIG cathode is modified with RGO/MWCNTs and silver oxide (Ag_2O) nanocomposites for the reduction of oxygen. The assembled biofuel cell exhibited a linear peak power response up to 18 mM glucose with sensitivity of 0.63 µW mM^{-1} cm^{-2} and exhibited good linearity ($r^2 = 0.99$). The glucose biofuel cell showed an open-circuit voltage of 0.365 V, a maximum power density of 11.3 µW cm^{-2} at a cell voltage of 0.25 V, and a short-circuit current density of 45.18 µA cm^{-2} when operating in 18 mM glucose. Cyclic voltammetry revealed the bioanode exhibited similar linearity for the detection of glucose. These results demonstrate that LIG based bioelectrodes offer great promise for diverse applications in the development of hybrid biofuel cell and biosensor technology.**

Keywords—LASER induced graphene, catalytic activity, self-powered biosensor, glucose biofuel cell.

I. INTRODUCTION

Self-powered biosensors (SPBs) are analytical tools in which the generated energy is proportional to the concentration of a specific analyte. SPBs have the potential to replace current conventional biosensors in real applications with several advantages including simple configurations (two electrodes), no external power sources, and ease of miniaturization and fabrication [1-3]. The development of self-powered biosensor for practical applications are limited by poor specificity to the target molecule, thereby resulting in limited conversion of energy and low output energy [4]. Efforts have been employed to develop SPBs by incorporating catalysts and nanomaterial interfaces [5]. Chansaenpak et al. developed enzymatic self-powered glucose biosensor, where the anode is fabricated on the glassy carbon electrode modified with graphene and enzyme materials and the cathode used graphitic electrode with multiwalled carbon nanotubes integrated with enzyme [6]. The fabricated glucose SPB showed good linearity up to 7 mM but achieved low power density. Huang et al. used Pt-Ir and conductive carbon black integrated with mediator and enzyme for bioanode and carbon cloth integrated enzyme as biocathode. The developed SPB demonstrated good linearity up to 10 mM glucose but exhibited lower power density [7]. Bucky paper based self-powered glucose sensor was developed by Kulkarni et al. Both bioanode and cathode fabricated on Bucky paper and the fabricated SPB showed high power density, but it exhibited a limited linear range [8]. Recently, laser-induced graphene (LIG) developed on polymeric materials via a LASER source have been used to create porous graphene material [9, 10]. However, due to its porous structure and weak adherence to its carbon precursor, LIG sheets exhibit poor electrochemical performance [11]. To address this limitation, the LIG surface is modified with carbon-based nanocomposites and other 2D nanomaterials [12-14].

Here in, a hybrid biofuel cell is fabricated on polyimide platform by facile one step laser scribed technique. The formed porous graphene is modified using reduced graphene oxide (RGO) and multiwalled carbon nanotubes (MWCNTs) nanocomposite to improve the electrical conductivity and stability of the LIG. The as-fabricated platform LIG/RGO-MWCNTs is employed as the bioelectrode substrates. The bioanode comprised pyrroloquinoline quinone-glucose dehydrogenase (PQQ-GDH) immobilized on LIG/RGO-MWCNTs surface via a heterobifunctional crosslinking agent, 1-pyrenebutanoic acid, succinimidyl ester (PBSE). PBSE is applied to the biocathode to link the Ag_2O nanocomposite layer and mediate electron transfer. The physiological characteristics of the anodic and cathodic nanomaterials were evaluated using field emission scanning electron microscopy (FESEM). The electrochemical performance was characterized using linear sweep voltammetry and cyclic voltammetry.

II. MATERIALS AND MATHODS

A. Chemicals

Silver nitrate, polyethylene glycol (6000), sodium phosphate monobasic, sodium phosphate dibasic, glucose, were procured from Sigma-Aldrich, USA. Multi-walled carbon nanotubes were procured from US Research Nanomaterials, USA and graphite oxide was obtained from ACS Material, USA. 1-1-pyrenebutanoic acid, succinimidyl ester (PBSE) and pyrroloquinoline quinone-glucose dehydrogenase (PQQ-GDH) was procured from Anaspec Inc. and Toyobo Co. Ltd, respectively. Polyimide film (thickness = 50 µm) was purchased from amazon marketplace. All stock solutions were prepared with ultrapure water (resistivity $\geqslant$ 18.2 M Ω -cm).

B. Synthesis of RGO/MWCNTs composites

The RGO/MWCNTs composite was synthesized according to the published article [15]. Briefly, 21 mg of multiwalled carbon nanotubes (MWCNTs) and 39 mg of reduced graphene oxide (RGO) were added into 30 ml of ulrapure water. The solution of composite was sonicated for 30 minutes using horn sonicator and then, poured into teflon-lined autoclave. The autoclave was placed inside the convection oven and allowed to heat up to 180 ºC for 3 h. The resulting cylindrical structured

The research presented in this article was supported by the National Science Foundation Award #1921364 and #1925806.

composite was added into 1 M acetic acid and allowed to disperse and functionalize for 5 h, after which the dispersed composite mixture was filtered and rinsed with ultrapure water until a pH of 7 was obtained. The composite material was dried overnight in a vacuum oven at 95 ºC. A uniform suspension of the dried composite platelets (1.25 mg/ml) was garnered upon exfoliation into dimethylformamide (DMF) and ultrapure water (1:1) mixture after 3 h.

C. *Fabrication LIG platform*

Polyimide tape (l = 15 mm) was adhered to polystyrene to provide structure integrity for handling. The taped substrate was cleaned in ethanol followed by ultrapure water. The polyimide film was engraved to form 3D graphene on the designated area (4x4 mm^2) using BOSS LS-1616 CO_2 pulsed laser (speed 200 mm/s, pass-1, layer- black, power max-25%, min power 25%). The fabricated LIG platform was used to prepare the bioanode and biocathode. A schematic diagram is provided in Scheme 1.

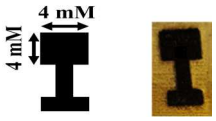

Scheme 1. A schematic diagram of the bioelectrode design and photomicrograph of LIG on the plastic platform.

D. *Fabrication of bioanode and biocathode*

10 µL of the RGO/MWCNTs nanocomposite was drop casted on the LIG platform and allowed to settle for 10 min and subsequently heated at 40 ºC for 20 min. This process was repeated trice to create a porous nanocomposite structure to enable interconnected networks of LIG sheets. The RGO/MWCNTs surface was further modified with 10 µL of PBSE (3 mg in to 250 mL DMSO) under dark condition and allowed to react overnight, rinsed in DMSO followed with phosphate buffered solution (PBS) rinse, and allowed to dry 10 min. 10 µL (1.5 mg in to 100µL 1 M $CaCl_2$) of PQQ-GDH was immobilized on the PBSE treated surface and allowed to dry at 4 ˚C in the refrigerator for several hours. For reducing enzyme leaching and increasing stability, 3 µL of 0.5% nafion was drop casted to coat the bioelectrode surface and placed in the refrigerator when not in use. The cathode was prepared using the RGO/MWCNTs/PBSE modified LIG substate modified with Ag_2O nanocomposite synthesized according to the previously published protocol [16]. The Ag_2O paste was applied to the PBSE surface and followed to dry in desiccator for several hours. The biocathode was coated with 3 µL of 5% nafion and placed in the desiccator until use.

III. RESULTS AND DISCUSSION

A. *Morphological characterization of LIG modified surface*

The surface morphology of the LIG and LIG modified surfaces were observed via FESEM. The porous and crumbled structure of LIG is observed after laser engraving of the polyimide film as shown in Fig. 1A. The types of graphene sheets formed on the surface are not tightly attached on LIG surface, thereby decreasing the overall electrode conductivity. To enhance the electrode conductivity, RGO/MWCNTs nanocomposite was casted on the LIG surface as shown in Fig. 1B. The RGO/MWCNTs layer created an interpenetrating network to improve conductivity and stability of the surface. PBSE was drop casted on the RGO/MWCNTs nanocomposite network to improve the carboxylic groups functionalization and to form a peptide bond with PQQ-GDH as shown in Fig. 1C. The pyrene groups attached on the surface of the RGO/MWCNTs modified surface via π-π interaction. The Ag_2O was applied to the PBSE modified surface as shown in Fig. 1D. Uniform distribution of Ag_2O is observed and this network of conductive materials provides excellent conduction pathways and electron transfer kinetics at the biocathode.

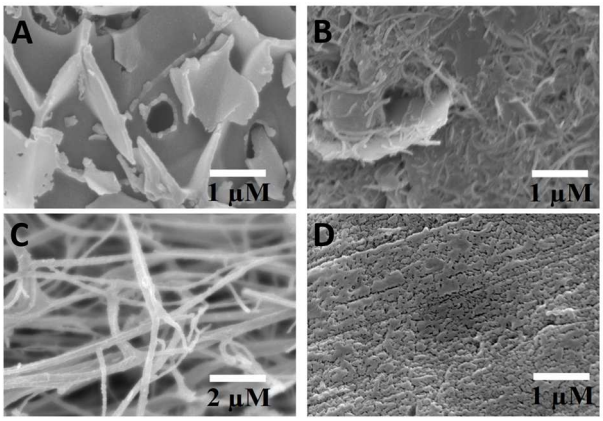

Fig. 1. FESEM images of (A) LIG, (B) LIG/RGO/ MWCNTs, (C) LIG/RGO/MWCNTs/PBSE, and (D) LIG/RGO/MWCNTs/PBSE/Ag_2O.

B. *Electrochemical charcterization of Bio-anode and cathode*

The electron transfer phenomena of the bioelectrodes were explored using electrochemical impedance spectroscopy (EIS). EIS spectra of LIG, RGO/MWCNTs, RGO/MWCNTs/PBSE, and RGO/MWCNTs/PBSE/PQQ/nafion bioelectrodes were recorded in 0.1 M PBS (pH 7.4) containing 5 mM $[Fe(CN)_6]^{3-}$ fitted with the Randles equivalence circuit model as shown in Fig. 2. These surfaces possess good electron transfer kinetics. The electron transfer resistance (R_{ct}) of the LIG electrode was

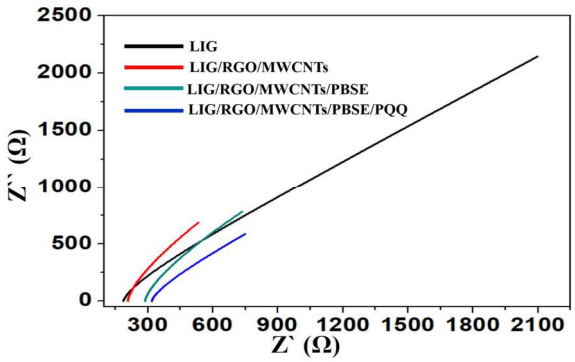

Fig. 2. Electrical impedance spectroscopy (EIS) of LIG, LIG/RGOMWCNTs, LIG/RGOMWCNTs/PBSE and PQQ-GDH modified electrodes in 0.1 M PBS (pH 7.4) containing 5 mM $Fe(CN)_6^{3-}$. 5 mVp-p at 0.1 Hz to 100 kHz.

higher than that of the modified LIG surfaces. The RGO/MWCNTs modified surface exhibited a R_{et} that is significantly higher, and a small increase was observed in R_{et} upon modifying the surface with PBSE. These results imply that the small barrier layer created was due to the pyrene groups. Upon immobilizing PQQ-GDH enzyme to increase the specificity energy conversion rate, the R_{et} increased, suggesting the immobilization of a protein layer on the surface.

The cyclic voltammetry (CV) was performed to observe the electrocatalytic process of glucose on the fabricated anodic electrode at different scan rate (20 -120 mV/s) as shown in Fig. 3. A good linear relationship with the square root of scan rate was observed for the anodic (r^2 = 0.998) and cathodic (r^2 = 0.997) scans. The result indicates that the fabricated bioanode is diffusion controlled.

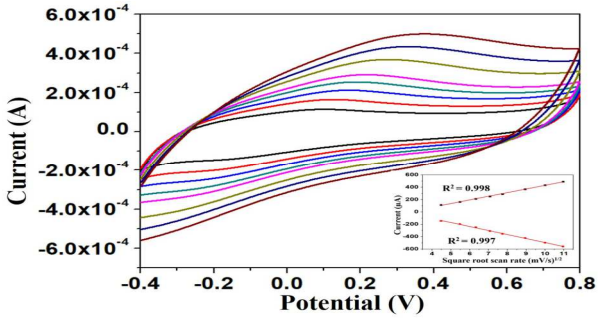

Fig. 3. CV voltammogram of the LIG/RGO/MWCNTs/ PBSE/PQQ/nafion in PBS containing 3 mM glucose at different scan rate (20, 30, 40, 50, 60, 80, 100 and 120 mV/s).

C. Electrochemical charaterization of biofuel cell

Polarization curves were generated using linear sweep voltammetry (LSV) as shown in Fig. LSV experiment was performed at 1 mV/s scan rate. Upon increasing the concentration of glucose, the current density and open circuit voltage increased. The corresponding power density curves are

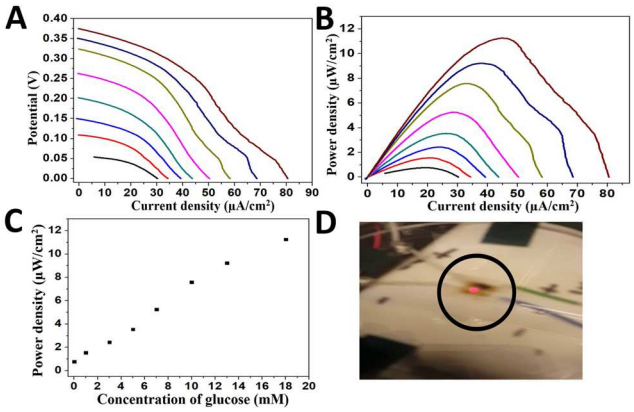

Fig. 4. (A) Polarization characteristics of the biofuel cell in various glucose concentrations (0, 1, 3, 5, 7, 10, 13, 18 mM), (B) The power curve as the functions of the current density, (C) The corresponding calibration curve, and (D) Illumination of an LED light with biofuel cell operating in 10 mM glucose via a voltage booster circuit.

shown in Figure 4B. The glucose biofuel cell exhibited an open-circuit voltage of 0.365 V, a maximum power density of 11.3 μW cm^{-2} at a cell voltage of 0.25 V, and a short-circuit current density of 45.18 μA cm^{-2} when operating in 18 mM glucose. The fabricated biofuel cell exhibited a sensitivity of 0.63 μW cm^{-2} mM^{-1} with a wide linear detection range up to 18 mM glucose (r^2 = 0.990) as shown in Fig. 4C. The electrical power generated from the fabricated biofuel cell was able to illuminate a light emitting diode (LED) interfaced to a voltage booster circuit as described elsewhere [18] and is shown in Fig. 4D. The results indicate that the hybrid biofuel cell have the potential to function as a SPB while converting the biochemical energy of glucose biomolecules.

CV of the bioanode was performed in the PBS with successive injection of different concentration of glucose as shown in Fig. 5A. The anodic current increased with increasing glucose concentration from 1 mM to 18 mM (r^2 = 0.987). The

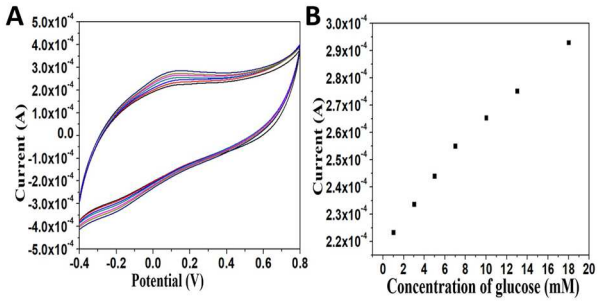

Fig. 5. (A) CV of the LIG bioanode in different concentration of glucose (1, 3, 5, 7, 10, 13 and 18 mM) and (B) corresponding calibration curve.

corresponding calibration curve of the anodic currents obtained at 0.15 V is shown in Fig. 5B. The bioanode demonstrated a sensitivity of 25.02 μA mM^{-1} cm^{-2}. The result is in accord with the result obtained from the power curves. The CV of biocathode was conducted in the presence and absence of O_2 saturated PBS not shown. The reduction current in the presence of O_2 is much higher than that in the absence of O_2 solution, which indicates that the biocathode was able to reduce oxygen to water, thereby completing the circuit in the biofuel cell assembly.

IV. Conclusions

Laser induced graphene was successfully fabricated on the polyimide tape and a hybrid glucose biofuel cell was constructed using a two bioelectrode design. The fabricated bioanode exhibited good electrocatalytic activity towards oxidation of glucose with the sensitivity of 25.02 μA mM^{-1} cm^{-2}. The biocathode showed good catalytic activity towards the reduction of oxygen. The hybrid biofuel cell system exhibited excellent catalytic activity towards oxidation of glucose and reduction of O_2 with the sensitivity of 0.63 μW mM^{-1} cm^{-2} and a wide detection range up to 18 mM (r^2 = 0.990). These results indicate that the glucose biofuel cell has the capability to sense glucose while functioning as a power source.

REFERENCES

[1] S. Hao, X. Sun, H. Zhang, J. Zhai, and S. Dong, "Recent development of biofuel cell based selfpowered biosensors," J. Mater. Chem. B, vol. 8, pp. 3393-3407, 2020.

[2] S. H. Huang, W. H. Chen, and Y. C. Lin, "A self-powered glucose biosensor operated underwater to monitor physiological status of free-swimming fish," Energies, vol. 12, pp. 1827, 2019.

[3] L. Fu, J. Liu, Z. Hu, and M. Zhou, "Recent advances in the construction of biofuel cells based self - powered electrochemical biosensors: A review," Electroanalysis vol. 30, pp. 2535 -2550, 2018.

[4] M. A. Pellitero, A. Guimer, M. Kitsara, R. Villa, C. Rubio, B. Lakard, M. L. Doche, J. Y. Hihnc, and F. J. del Campo, "Quantitative self-powered electrochromic biosensors." Chem. Sci., vol. 8, pp. 1995–2002, 2017.

[5] M. Grattieri, and S. D. Minteer, "Self-powered biosensors," ACS Sens. vol. 3, pp. 44−53, 2018.

[6] K. Chansaenpak, A. Kamkaew, S. Lisnund, P. Prachai, P. Ratwirunkit, T. Jingpho, V. Blay, and P. Pinyou, "Development of a sensitive self-powered glucose biosensor based on an enzymatic biofuel cell," Biosensors, vol. 11, pp. 16, 2021.

[7] S. H. Huang, W. H. Chen, and Y. C. Lin, "A Self-Powered Glucose Biosensor Operated Underwater to Monitor Physiological Status of Free-Swimming Fish,"Energies, vol. 12, pp.1827, 2019.

[8] G. Slaughter, and T. Kulkarni, "A self-powered glucose biosensing system," Biosens. Bioelectron., vol. 78, pp. 45-50, 2016.

[9] F. Mahmood, H. Zhang, J. Lin, and C. Wan, "Laser-induced graphene derived from kraft lignin for flexible supercapacitors," ACS Omega, vol.5, pp. 14611−14618, 2020.

[10] R. Ye, D. K. James, and J. M. Tour, Laser-induced graphene: From discovery to translation. Adv. Mater. vol. 31, pp. 1803621, 2019.

[11] U.S. Jayapiriya, P. Rewatkar, S. Goel, "Miniaturized polymeric enzymatic biofuel cell with integrated microfluidic device and enhanced laser ablated bioelectrodes," Int. J. Hydrog. Energy, vol. 46, pp. 3183-3192, 2021.

[12] F. Clerici, M. Fontana, S. Bianco, M. Serrapede, F. Perrucci, S. Ferrero, E. Tresso, and A. Lamberti, "In situ MoS2 decoration of laser-induced graphene as flexible supercapacitor electrodes," ACS Appl. Mater. Interfaces, vol. 8, pp. 10459−10465, 2016.

[13] S. Nasraoui, A. Al-Hamry, A. Anurag, P. R. Teixeira, S. Ameur, L. G. Paterno, M. Ben Ali, and O. Kanoun, "Investigation of laser induced graphene electrodes modified by MWNT/AuNPs for detection of nitrite," 16th International Multi-Conference on Systems, Signals & Devices (SSD 2019), Turkey, P.615, 2019.

[14] F. Clerici, M. Fontana, S. Bianco, M. Serrapede, F. Perrucci, S. Ferrero, E. Tresso, and A. Lamberti, "In situ MoS2 decoration of laser-induced graphene as flexible supercapacitor electrodes," ACS Appl. Mater. Interfaces, vol. 8, pp. 10459−10465, 2016.

[15] W. Ma, J. Zhu, Z. Wang, W. Song, G. Cao, "Recent advances in preparation and application of laser induced graphene in energy storage devices," Materialstoday Energy, vol. 18, pp. 100569, 2020.

[16] M. F. Hossain, and J. Y. Park, "Plain to point network reduced graphene oxide - activated carbon composites decorated with platinum nanoparticles for urine glucose detection," Sci. Report., vol. 6, pp. 21009, 2016.

[17] N. L. Yong, A. Ahmad, and A. W. Mohammad, "Synthesis and characterization of silver oxide nanoparticles by a novel method," Int. J. Sci. Eng. Res., vol. 4, pp. 155-158, 2013.

[18] M. Q. Hasan, R. Kuis, J. S. Narayanan, and G. Slaughter, "Fabrication of highly effective hybrid biofuel cell based on integral colloidal platinum and bilirubin oxidase on gold support," Sci. report. vol. 8, pp. 16351, 2018.